Available online on www.ijddt.com
International Journal of Drug Delivery Technology 2018; 8(1); 19-32
doi: 10.25258/ijddt.v8i01.11903
ISSN: 0975 4415

Research Article

Optimization of Redispersible Spray Dried Powder of Chitosan Coated Solid Lipid-Based Nanosystems

Munawiroh S Z[1, 2], Lipipun V[2], Ritthidej G C[2*]

[1]*Faculty of Mathematics and Sciences, Universitas Islam Indonesia, Yogyakarta, Indonesia*
[2]*Faculty of Pharmaceutical Sciences, Chulalongkorn University, Bangkok 10330, Thailand*

Received: 6th Oct, 17; Revised: 27th Jan, 18, Accepted: 4th Mar, 18; Available Online: 25th Mar, 2018

ABSTRACT
The present work describes the optimization of spray dried powder of solid lipid-based nanosystems to improve drug stability, surface modification and to obtain nanosystems after redispersion. Chitosan coated solid lipid nanoparticles containing bromocriptine mesylate (cBMSLN) were prepared by high pressure homogenization technique following by chitosan addition. For spray drying, response surface methodology with central composite rotatable design was to optimize 3 parameters: inlet temperature, pump rate and feed concentration. From regression analysis, powder yield, moisture content and size of redispersed nanoaggregates as responses were fitted well with linear, quadratic and quadratic equation models, respectively. Spherical powders with size of 4-5 µm and 70% yield were obtained at optimum parameters which were also used to prepare powder of chitosan coated nanostructured lipid carriers containing BM (cBMNLC). Amorphous characteristics were confirmed from powder XRD patterns and DSC chromatograms in all prepared powders. Redispersion of powders yielded nanosystems of some original nanosize and a greater portion of larger size. Smoother surface of NLC systems was observed, so was with chitosan coating. Drug entrapment was >85% but significantly decreased in chitosan coated formulations while drug retention after spray drying showed opposite results. After storage, spray dried powder could retain higher drug content than the original nanosystems. Obviously, NLC systems had better drug stability results than SLN systems. It could be concluded that redispersible spray dried powders of chitosan coated lipid-based nanosystems especially NLC systems were successfully obtained with surface modification, nanoaggregate size range and improved drug stability.

Keywords: Solid lipid nanoparticles, nanostructure lipid carriers, chitosan, spray drying, optimization, redispersion, bromocriptine mesylate.

INTRODUCTION

Recently, redispersion of dried nanosystems for oral administration has gained much attention[1]. Transformation of liquid nanosystems into powders was to overcome aging and long term stability problems including to improve handling. Moreover, the powders can be further manufactured as conventional solid dosage forms such as tablets and capsules for better patient compliance. These solid nanosystems can be achieved by several techniques with the addition of carriers such as maltodextrin and lactose[2], trehalose[3], charge surfactant[4] and porous carrier[5]. Redispersion efficiency can partially or totally recover the size of original nanostructure depending on drying conditions and original nanosystems[6].

Spray drying, the most widely used drying process with advantages of low cost and less time consuming is able to produce spherical powder with narrow distribution, uniformed drug content and amorphous state[6, 7]. However, due to limitations and high number of critical process parameters[8], formulation and process control require particular attention that a prudential optimization design is practical to minimize total number of experiments.

Meanwhile, lipid-based nanosystems are able to enhance oral absorption[9]. Their gastrointestinal absorption includes lymphatic transport bypassing hepatic metabolism[5] and consequent transport across blood brain barrier[10]. Solid lipid nanoparticles (SLN) and nanostructured lipid carriers (NLC) are two kinds of lipid-based nanosystems that have potential advantages of low toxicity, high loading capacity of water insoluble drug, sterilization ability, best production scalability[11]. Improved drug loading and stabilized drug incorporation during storage are additional advantages of NLC[12]. Adversely, lipid-based nanosystems could be easily opsonized by plasma opsonins and uptaken by the mononuclear phagocyte system (MPS)[13]. Surface modification by hydrophilic compounds could prolong SLN blood circulation such as Pluronic F68[14], poloxamer 188[15], polyethylene glycol[16] and polysorbate 80[17]. Recently, chitosan, a biopolymer, not only improves blood circulation upon SLN surface modification[18] but can increase oral absorption by opening tight junction of intestinal epithelial and be specific to brain targeting[19-21]. Therefore, spray dried powder of chitosan coated solid lipid-based nanosystems has been attempted to develop in

**Author for Correspondence: garnpimol.r@chula.a.cth*

order to obtain lipid nanoparticles upon mild agitation with water.

Bromocriptine mesylate (BM), a drug used for Parkinson's disease is reported to have low oral bioavailability due to low solubility and high hepatic metabolism[5]. In present study, SLN containing BM was prepared prior to addition of chitosan (cBMSLN), then spray dried and optimized to obtain nanosize of redispersed aggregates using maltodextrin as stabilizer and drying aid. Similarly, NLC system of cBMNLC and those without chitosan were prepared and then spray dried with the optimized conditions. Initial lipid-based nanosystems, their spray dried powders and redispersions were characterized and compared. The entrapment efficiency in nanosystems and drug retention in powders were assessed. Drug stability of capsules containing spray dried powders was compared to initial nanosystems.

MATERIALS AND METHODS

Materials

Bromocriptine mesylate (BM) *(*Sigma Chemical Co, St Louis, MO, USA) and low molecular weight chitosan (50,000Da with 75-85% deacetylation) (Sigma-Aldrich, Germany) were purchased from Sigma, Thailand. Tristearin (Dynasan 118), trimyristin (Dynasan 114) were obtained from TCI Japan. Ethylene oxide/propylene oxide block copolymer (Pluronic F127), sorbitan polyoxyethylene monooleate (tween 80) and sorbitan monooleate (span 80), were from BASF, NJ, USA, VWR International Ltd., UK and Fluka Chemika, Germany, respectively. Ultrapure water (Maxima UltraPure Water, Elga-Prima Corp, UK) with a resistivity greater than 18 MΩ/cm was used to prepare all preparations.

Methods

Preparation of cBMSLN

BMSLN containing 0.025% (w/w) of BM, 1% of tristearin:trimyristin 7:3 as lipids and 2% w/w of tween 80:Pluronic F127:span 80 2:1:1 as surfactants were prepared by hot high pressure homogenization technique. Briefly, lipids and span 80 were melted at 10ºC above their melting points and BM in 1 ml ethanol was then dissolved in this lipid phase. The aqueous phase consisting of hot ultrapure water (80ºC), tween 80 and Pluronic F127 was added to lipid phase. The mixture was homogenized using ultra Turrax (IKA-Werke GmbH & Co., Staufen, Germany) at 10,000 rpm for 5 minutes to form coarse dispersion and then homogenized (Emulsiflex-B3, Avestin Inc., Canada) at pressure of 1000 bars for 5 cycles and then cooled under refrigerated temperature to obtain BMSLN. To form cBMSLN, 10 ml BMSLN was added consecutively dropwise to an equal volume of 0.5% chitosan solution (in 1% acetic acid). Incubation to equilibrate coating was performed at room temperature (25ºC) for 30 min prior to spray drying process.

Optimization of spray dried powder of cBMSLN (cBMSLN powder)

Maltodextrin was added to the prepared cBMSLN at varied concentrations according to the total feed concentrations in formulations and then spray dried (Mini Büchi B-290, Büchi, Switzerland) according to experimental design and at 320 l/h of gas flow rate and 100% of aspiration. The obtained powders were then stored in a humidity controlled cabinet for a 48 h period prior to their characterization.

Experimental design Response surface methodology (RSM) was employed for optimization[22]. Three factors and two levels central composite rotatable design 2^3 principal[23] was selected to study the effect of 3 independent processing variables, inlet temperature (X_1), pump rate (X_2) and feed concentration (X_3). Responses were powder yield, moisture content and size of redispersed nanoaggregates. Eight full factorial design augmented by 12 "star" points (6 axial points and 6 replicated center points) was to evaluate each variable (X_1-X_3). The levels of each vaiable were obtained from preliminary experiments (Table 1).

Design containing 20 runs was generated and analyzed by statistical software package Design-Expert V. 8 (StatEase Inc., USA). Effects and interactions between variables were calculated.

Experimental responses were the results of individual influence and interactions of 3 independent variables following polynomial model:

$$Y = b_0+bX_1+b_2X_2+b_3X_3+b_{11}X_1^2+b_{22}X_2^2+b_{33}X_3^2+b_{12}X_1X_2 +b_{13}X_1X_3+b_{23}X_2X_3\ldots\ldots\ldots \quad (1)$$

where Y was the measured response, b_0 the intercept term, $b_i's$ (for i = 1–3) were the linear effects, $b_{ii}'s$ were the quadratic effects, $b_{ij}'s$ (for i,j = 1–3, $i < j$) were the interaction between the i and j variables. Statistically significant at F ratio ($\alpha < 0.05$) and statistically insignificant lack of fit ($\alpha > 0.05$) were to select model equation[22]. The criteria of optimization were determined by maximum powder yield, minimum moisture content and minimum size of redispersed nanoaggregates.

Percentage of powder yield Powder sample was thoroughly collected from collector chamber of the spray dryer and weighed. The % powder yield was calculated following the equation,

$$\%\,powder\ yield = \frac{W_{obtained}}{W_{initial}} \times 100\% \quad \ldots\ldots\ldots\ldots\ldots\ldots (2)$$

$W_{initial}$ was the mass of initial solid part in the sample and $W_{obtained}$ was the mass obtained from drying process.

Moisture content Powder sample of about 0.5 g was weighed. The residual moisture content was determined via loss-on-drying using a Mettler Toledo Deluxe Halogen Moisture Analyzer HR83 (Mettler-Toledo, Belgium) and calculated as % moisture content.

Size of redispersed nanoaggregates One hundred mg of dried powder was redispersed in 10 ml purified water under gentle agitation prior to determination of size and polydispersity index (PI) by a Nano-ZS zetasizer (Malvern Instruments, Malvern, UK) at 25ºC. The zeta potential of the redispersion was also consequently measured using zeta clear cells. Each measurement was made in triplicate.

Table 1: Parameters and coded level of variables for experimental design.

Variable	Processing parameters				
	Low level (-)	Center point (0)	High level (+)	Low level of axial point (-α)	High level of axial point (+α)
X_1: Inlet temperature (^{0}C)	115	137.5	160	100	175
X_2: Pump rate (%*)	16	24	32	10.6	37.4
X_3: Feed concentration (%)	10	20	30	3.2	36.8

* 1 % of pump rate equals to 0.5 ml/min

Preparation of spray dried powder of cBMNLC (cBMNLC powder)

The cBMNLC was prepared by the same procedure as cBMSLN with similar formulation except tristearin:trimyristin:castor oil 2:1:2 was used as lipid components. Spray drying was following the optimum conditions obtained from section 2.2.2 and then the powder was similarly characterized. BMSLN and BMNLC without chitosan were also prepared, spray dried and used for comparison.

Solid state characterization

DSC analysis Solid parts of cBMSLN and cBMNLC were obtained by ultracentrifugation and dried in a desiccator. Their physical state was characterized by a differential scanning calorimeter (DSC 2000A, Mettler Toledo TA, USA) and compared to their physical mixture. Sample of about 5 mg was sealed in standard aluminum pan with lid and then scanned at a heating temperature speed of 5°C/min with protection by pure dry nitrogen gas at 60 ml/min. Indium was used as standard reference material to calibrate the temperature and energy scale of the DSC instrument[24]. The physical state of BM in spray dried samples was also characterized and compared to their physical mixtures and each solid component in formulation.

Powder X- ray diffraction (PXRD) analysis The spray dried samples were characterized for their crystallography structure by PXRD (Siemens D5000, Germany) as well as other solid components in the formulation (maltodextrin, tristearin, trimyristin and Pluronic f127). The physical mixture of BM with cSLN and cNLC powder were also characterized. A voltage of 40 kV and a current of 50 mA for the generator were applied with Cu as tube anode material. The solid was exposed to a Cu-K radiation, over a range of 2θ angles from 5° to 30°, at sampling interval of 0.02°[25].

Morphology of spray dried powders and their redispersions

Scanning electron microscopy (SEM) analysis Shape and surface morphology of powders of BMSLN, cBMSLN, BMNLC, cBMNLC were examined under a scanning electron microscope (SEM, Hitachi S-4100) after gold palladium coating onto the powders using an ion coater.

Transmission electron microscopy (TEM) analysis Each powder sample was diluted 10-fold with ultrapure water onto a copper grid followed by negative staining with 1% phosphotungstic acid and then kept in a desiccator for 2 h to get rid of excess water[26]. The morphology of redispersions was characterized under a transmission electron microscope (TEM) (model JSM-6700F (JEOL, USA) and compared to samples before spray drying.

Physical properties of cBMSLN and cBMNLC spray dried powders

Particle size measurement Size distribution of spray dried powder was determined by a Scirocco 2000 dry powder system provided with a Mastersizer 2000 using laser diffraction (Malvern Mastersizer 2000, UK). The refractive index of lipid was 1.33, the absorption value was 0.1 whereas the refractive index of maltodextrin was 1.43. The size distribution was determined by volume distribution and expressed as mean [d(4,3)]. The width of the droplet size distribution was expressed by the span value:

$$span = \frac{d(v,0.9) - d(v,0.1)}{d(v,0.5)} \quad \text{……..(3)}$$

where $d(v,0.9)$, $d(v,0.5)$ and $d(v,0.1)$ were the diameters of 90%, 50% (median) and 10% volume distribution, respectively.

Powder flowability Carr's compressibility index (CI) to characterize powder flowability, was determined by the following equation.

$$CI = \frac{\rho_{tap} - \rho_{bulk}}{\rho_{tap}} \times 100\%$$

…… (4)

where ρ_{bulk}, the bulk density, was the weight of bulk powder divided by the bulk volume, ρ_{tap}, the tapped density was the weight of bulk powder divided by the tapped volume obtained from tapping the bulk using in-house densitometer up to 1200 taps. The CI values below 25 indicated free-flowing powder and values above 40 indicated poor flowability[27].

Chemical analysis

BM content was determined by HPLC method with some adjustments[28]. An HPLC (Shimadzu model LC-8A, Japan) system consisted of two pumps (Shimadzu LC-20AD, Japan) and a variable wavelength UV/Vis-detector (Shimadzu SPD-20A/AV, Japan) was operated at 300 nm. The BDS Hypersil C-18 reverse-phase column (25×0.46 cm, Thermo Scientific, USA) packed with 5 µm particles was used. The flow rate was 1.0 ml min^{-1} and the column temperature was room temperature at 25ºC. The samples were injected at 20 µl loop. The mobile phase was a mixture of methanol and buffer ammonium (70:30). The retention time was 6.19 to 6.30 min. The calibration curve was found linearly in the range of 2.0-10.0 µg/ml.

Table 2: A rotatable central composite experimental design and three responses; yield, moisture content and size of redispersed nanoaggregates.

Standard order	Run	X_1	X_2	X_3	Design	Inlet temp. (^{0}C)	Pump rate (%)	Feed conc. (%)	Yield (%)	Moisture content (%)	Size of redispersed Nanoaggregates (nm)
12	1	0	0	0	Center point	137.5	24.0	20.0	55.20	4.09	1448
3	2	-1	1	1	Factorial	115.0	32.0	10.0	61.30	8.32	311
9	3	0	0	0	Center point	137.5	24.0	20.0	55.80	5.42	1586
1	4	-1	-1	-1	Factorial	115.0	16.0	10.0	73.70	5.13	254.6
2	5	1	-1	-1	Factorial	160.0	16.0	10.0	77.80	5.38	282.2
6	6	1	-1	1	Factorial	160.0	16.0	30.0	42.67	5.40	886.7
10	7	0	0	0	Center point	137.5	24.0	20.0	55.80	5.15	1445
4	8	1	1	-1	Factorial	160.0	32.0	10.0	64.80	4.86	293.7
8	9	1	1	1	Factorial	160.0	32.0	30.0	38.93	5.92	1297
11	10	0	0	0	Center point	137.5	24.0	20.0	53.10	6.86	1220
5	11	-1	-1	1	Factorial	115.0	16.0	30.0	40.50	8.07	1365
7	12	-1	1	1	Factorial	115.0	32.0	30.0	31.00	3.74	834.6
14	13	1.68	0	0	Star axial	175.3	24.0	20.0	60.15	7.13	1378
13	14	-1.68	0	0	Star axial	99.7	24.0	20.0	53.50	6.79	737.5
18	15	0	0	1.68	Star axial	137.5	24.0	36.8	39.36	6.62	732.7
15	16	0	-1.68	0	Star axial	137.5	10.6	20.0	61.45	3.18	1298
17	17	0	0	-1.68	Star axial	137.5	24.0	3.2	85.56	4.89	396
19	18	0	0	0	Center point	137.5	24.0	20.0	57.45	4.91	1288
20	19	0	0	0	Center point	137.5	24.0	20.0	56.00	5.13	1438
16	20	0	1.68	0	Star axial	137.5	37.4	20.0	53.35	4.65	701.4

Drug entrapment efficiency (DEE) Free BM in the aqueous phase of SLN and NLC samples before spray drying was separated by ultrafiltration centrifugation technique[29]. Briefly, 3 ml of sample dispersion was placed in the upper chamber of a centrifuge tube matched with an ultrafilter (Amicon ultra, Millipore Co., USA, MWCO 10kDa) and centrifuged for 30 min 4000 rpm at 4ºC (Eppendorf 5804R, Germany). One ml of ultrafiltrate which contained the free BM (W_{free}) was diluted with methanol and then determined by aforementioned HPLC method.

The total drug content (W_{total}) in BMSLN, cBMSLN, BMNLC or cBMNLC was obtained as follows: aliquots of 1 ml sample dispersion were diluted appropriately by methanol with 0.1% of Triton™ X100 and incubated in a shaker for 1 h to dissolve the lipid ingredient and then filtrated through 0.45 µ membrane filter. The resulting solution was analyzed by HPLC. DEE was calculated by the following equation:

$$DEE(\%) = \frac{W_{total} - W_{free}}{W_{total}} \times 100\% \quad \text{.....} \quad (5)$$

Drug retention (DR) An accurate weight of about 1.0 g of spray dried powder was redispersed in 10 ml of Milli-Q H2O in capped glass vials. Then 1 ml of redispersion was treated following the total drug content procedure to obtain the BM concentration ($BM_{after\ spray\ drying}$). The DR was calculated as the amount of BM in the spray dried powder relative to the amount of BM in the SLN or NLC before spray drying ($BM_{before\ spray\ drying}$):

$$DR(\%) = \frac{BM_{after\ spray\ drying}}{BM_{before\ spray\ drying}} \times 100\% \text{.....} \quad (6)$$

Preliminary stability study

Each sample was weighed equivalent to 3 mg BM and filled in size #2 hard gelatin capsules, packed in aluminum strips and stored at 25±2°C in a desiccator for 3 months. Drug content was determined at Day 0, 30, 60 and 90 compared to their corresponding chitosan coated lipid-based nanosystems[30] by HPLC analysis. Each study was performed in triplicate.

RESULTS AND DISCUSSIONS

Experimental design

Results of three dependent variables from experimental design, % powder yield, % moisture content and size of redispersed nanoaggregates were ranged from 31.00-85.56, 3.18-8.32 and 254.6-1586 nm, respectively (Table 2).

The fitted models of equations chosen from RSM were based on the results of statistical analysis shown in Table 3. The significant F ratio (α <0.05) of model *p* value and non-statistically significant lack of fit (α > 0.05) of three models indicated that the model equations fitted the data well. The responses of powder yield, moisture content and size of redispersed nanoaggregates were fitted with linear,

Table 3: Statistical analysis of experimental design and p-values of coefficient (95% confidence interval) of the regression fitting model design.

Factor	Yield (%)	Moisture content (%)	Size of redispersed nanoaggregates (nm)
Model p-value	< 0.0001	0.0400	0.0108
R^2	0.9668	0.7437	0.8208
Lack of fit test value	0.0837	0.5463	0.0501
Model	Linear	Quadratic	Quadratic
X_1	0.0152	ns	ns
X_2	0.0002	ns	ns
X_3	< 0.0001	ns	0.0094
X_1 X_2	-	ns	ns
X_1 X_3	-	ns	ns
X_2 X_3	-	0.0315	
X_1^2	-	0.0206	ns
X_2^2	-	ns	ns
X_3^2	-	ns	0.0033

ns: non-significant (p>0.05)

quadratic and quadratic models, described in Equations 7, 8 and 9, respectively.

Powder yield = $83.76 + 0.009 * X_1 - 0.48 * X_2 - 1.48 * X_3$ ..... (7)

Moisture content = $30.15 - 0.42 * X_1 + 0.41 * X_2 - 0.04 * X_3 + 0.001 * X_1 X_2 + 0.01 * X_1 X_3 - 0.01 * X_2 X_3 + 0.001 * X_1^2 - 0.007 * X_2^2 + 0.002 * X_3^2$ ..... (8)

Size of redispersed nanoaggregates = $-6253.31 + 73.48 * X_1 + 42.91 * X_2 + 169.03 * X_1 X_2 - 0.01 * X_1 X_3 - 0.29 * X_2 X_3 - 0.31 * X_1^2 - 2.75 * X_2^2 - 3.30 * X_3^2$ ..... (9)

where X_1, X_2 and X_3 were inlet temperature, pump rate and feed concentration, respectively.

Validation of model equations

Three diagnostic plots generated by Design Expert V.8. 05 were employed to confirm the fit models: 1) normal probability plot of studentized residuals, 2) studentized versus predicted values and 3) Cook's distance of run number. The first diagnostic plots of all models described straight line indicating normally distribution residual (Figures 1.1a-c). The unrevealed pattern of the second diagnostic plots of three models and values of less than ±3 (Figures 1.2a-c) indicated that models were correct and the assumptions to build the models were satisfied[22] while the third diagnostic plots of all responses (Figures 1.3a-c) were less than 1. The result indicated that run number did not influence the data responses[31]. Therefore, these models of three responses generated from RSM with the central composite design were applicable for following prediction of optimum condition set for spray drying of cBMSLN.

Selection of optimum parameters

The Design Expert.V.8.05 generated solutions to meet the criteria of maximum powder yield, minimum moisture content, and minimum size of redispersed nanoaggregates and the optimum parameters i.e. inlet temperature, pump rate and feed concentration were found to range from 115-118.68ºC, 16-16.21% and 10-10.56%, respectively, and the highest desirability of 0.8833066 was from 115ºC, 16% and 10%, respectively.

Effects of inlet temperature, pump rate and feed concentration on responses

Figure 2 shows the 3D graphs generated from Design Expert V.8.05 informing the influence of inlet temperature, pump rate and feed concentration. The *p* values of coefficient of the regression fitting model designed from Table 3 and the value of each coefficient in Equations 7, 8 and 9 were depicted to observe the influence of each parameter.

Effects on % powder yield Linear influence of inlet temperature, pump rate and feed concentration on % yield was significant ($p<0.05$), shown as 0.0152, 0.0002 and <0.0001, respectively (Table 3). The positive effect of inlet temperature and negative effect of pump rate and feed concentration were depicted from values of coefficient number in Equation 6.

Increasing inlet temperature led to a slight increase in % powder yield at both low and high levels of feed concentration (Figure 2.1a) or pump rate (Figure 2.1b) possibly due to increasing the rate of heat transfer. Higher efficient air drying at high temperature led to increase in potential (pressure and concentration) difference[32]. In addition, lower powder loss with exhausted air and residue accumulation were observed at the higher inlet temperature resulting higher powder yield[33].

In contrast, increasing pump rate resulted in lower powder yield at low and high inlet temperatures (Figure 2.1b) and feed concentrations (Figure 2.1c) due to incomplete evaporation and condensation of dispersion on chamber wall[34]. Moreover, lower yield was also obtained from higher feed concentration (Figure 2.1a) which was accordingly related to higher viscosity which impaired the effectiveness of drying process[35].

Effects on moisture content

The 3 spray drying variables did not have linearly significant effect on moisture content. Only interaction of feed concentration and pump rate, and quadratic of inlet temperature contributed a significant effect (Table 3). According to Equation 8, the pump rate had positive effect on moisture content, while the negative effect was from inlet temperature and feed concentration.

At low feed concentration, pump rate had positive effect, while opposite effect was seen at high feed concentration (Figure 2.2). The negative effect of interaction between feed concentration and pump rate was related to drying process. Higher viscosity from higher feed concentration and shorter time contact of feed to heat from higher pump rate would lead to less water evaporation[36].

Figure 2 Response surface plots: 1. powder yield; (a) effects of inlet temperature and feed concentration, (b) effects of feed rate and inlet temperature, (c) effects of inlet

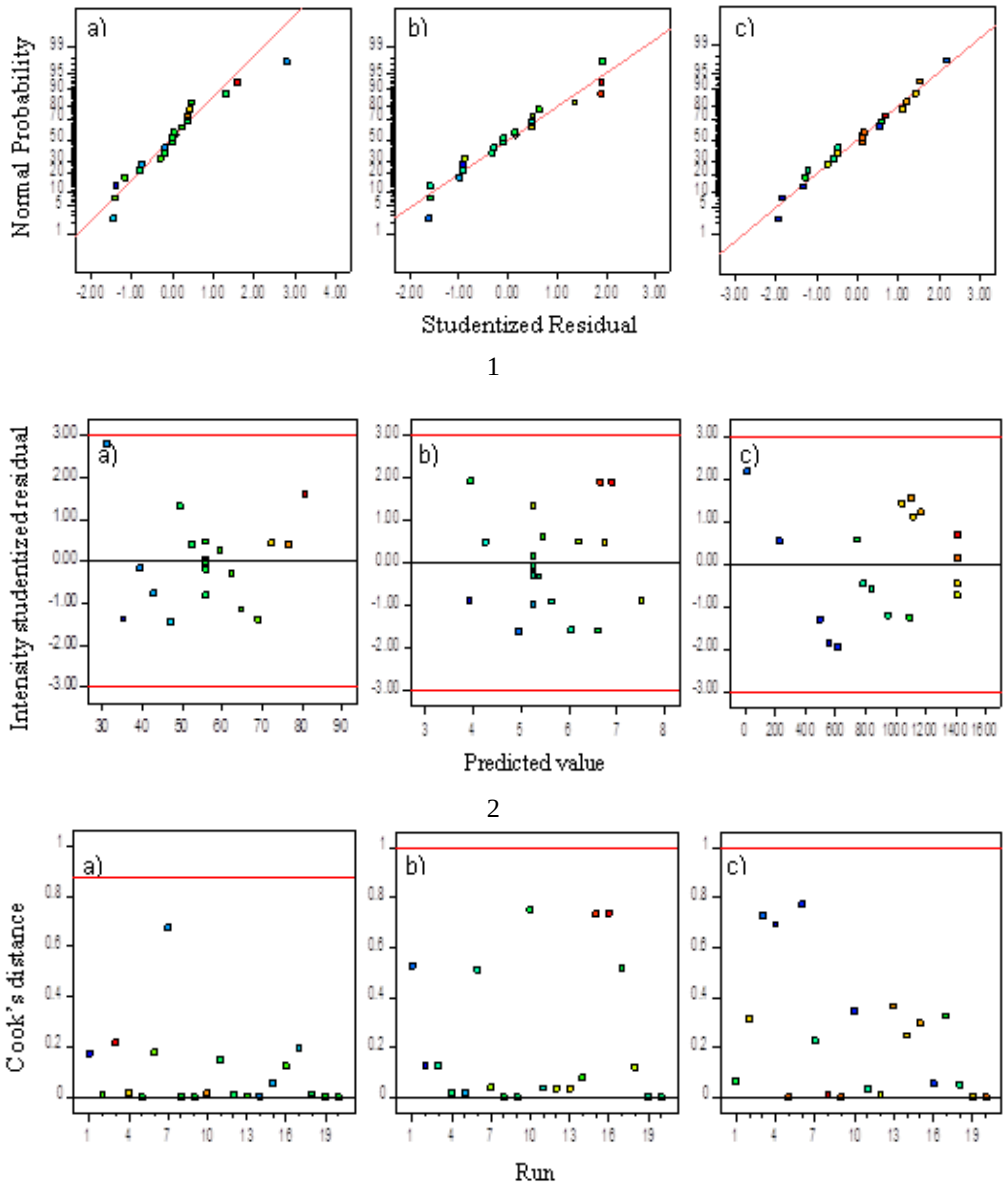

Figure 1: Normal % probability plots of studentized residuals (1), plots of predicted values versus studentized residual (2), and Cook's distance plots of run number (3); a) powder yield, b) moisture content and c) size of redispersed nanoaggregates.

temperature and feed rate; 2. moisture content; (a) effects of feed concentration and feed rate, 3. size of redispersed nanoaggregates; (a) effects of inlet temperature and feed concentration, (b) effects of feed concentration and feed rate.

Effect on size of redispersed nanoaggregates Table 3 shows that feed concentration and temperature had linearly and quadratically significant effect on size of nanoaggregates, respectively. Increasing the feed concentration had a markedly positive effect on nanoaggregate size at both low and high temperatures (Figure 2.3a) while lowering feed concentration led to less amount of dried substance, thus less cohesion or agglomeration thus rendering smaller size of nanoaggregates[37].

The effect of pump rate on size of nanoaggregates was negative. Smaller size was obtained when the pump rate increased both at low and high levels of feed concentration (Figure 2.3.b). It was probably assumed that faster pump rate rendering shorter contact but higher collision among particles might impair the formation of large nanoaggregates**.**

Solid state characterization

DSC characterization

The crystalline BM displayed a single strong endothermic peak at 219.67°C and exothermic peak at 215.33°C (Figure 3a) while the lipid components of formulation, tristearin, trimyristin, Pluronic F127, showed exothermic peak at 75.67°C, 60.33°C and 59.67°C (Figures 3b-d), respectively. As an amorphous compound, maltodextrin showed a slight exothermic large broad band from 32.67°C

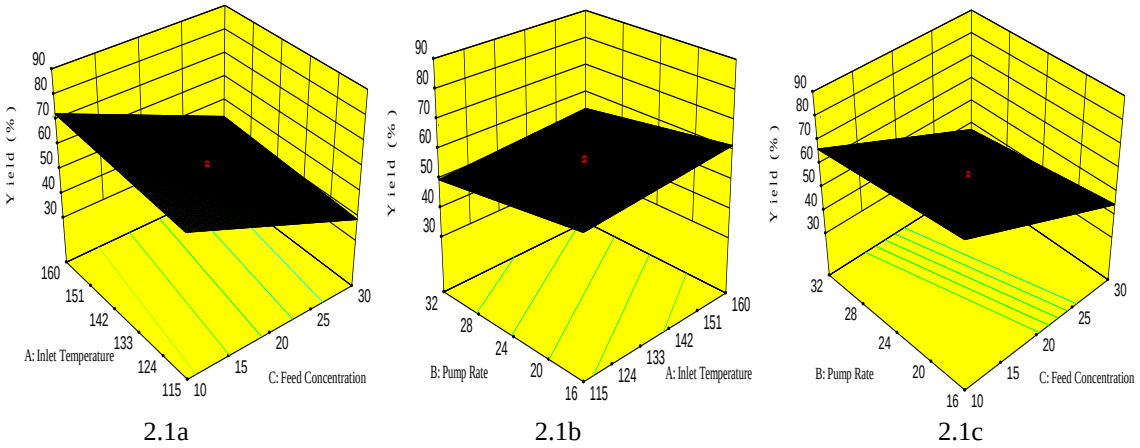

2.1a 2.1b 2.1c

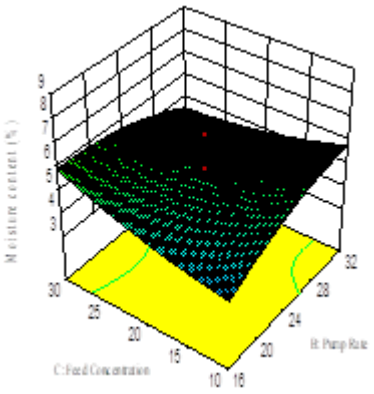

2.2a

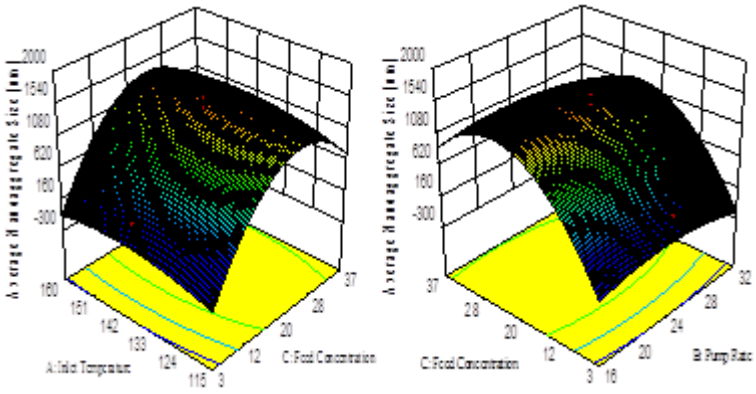

2.3a 2.3b

to 211.67°C (Figure 3e). The physical mixture of all components in the formulation still showed a sharp exothermic peak at 71.33°C and two exothermic peaks at 55.33°C, 46.33°C which associated with the shifted peaks of tristearin, trimyristin and Pluronic F127, respectively (Figures 3f and 3h). The DSC thermograms of both cBMSLN and cBMNLC powders showed that the exothermic peaks of crystalline components were totally disappeared, similarly to that of maltodextrin (Figures 3g and 3i). The decreasing enthalpy values which represented by exothermic peaks indicated the less ordered crystal or amorphous substance that required less energy to overcome lattice force[38, 39]. This phenomenon suggested that the obtained spray dried powders existed in amorphous state and caused an ease in dispersion.

PXRD characterization

The PXRD pattern of BM showed intense and sharp peaks at 12.434°, 13.234°, 14.286°, 15.727°, 16.734°, 17.146°, 20.920°, 22.338° and 23.504° (Figure 4a) indicating of crystalline nature whereas maltodextrin had no sharp peak diffraction (Figure 4b). For tristearin, trimyristin and Pluronic F127, their peaks were at 5.914°, 19.341°, 23.161° and 24.236° (Figure 4c), 7.424°, 16.940°, 19.387°, 23.230° and 24.076° (Figure 4d) and 19.204°, 23.390° and 26.363° (Figure 4e), respectively. The crystalline peaks of lipid components still appeared with decreasing intensities in their physical mixture (16.573°, 16.962°, 19.341°, 23.184° and 24.121°) but no peak of BM was observed (Figures 4f and 4h) probably due to low concentration of BM in the mixtures. Moreover, lower lipid peak intensity in NLC systems was noted owing to liquid composition in the systems. All diffraction peaks of cBMSLN and

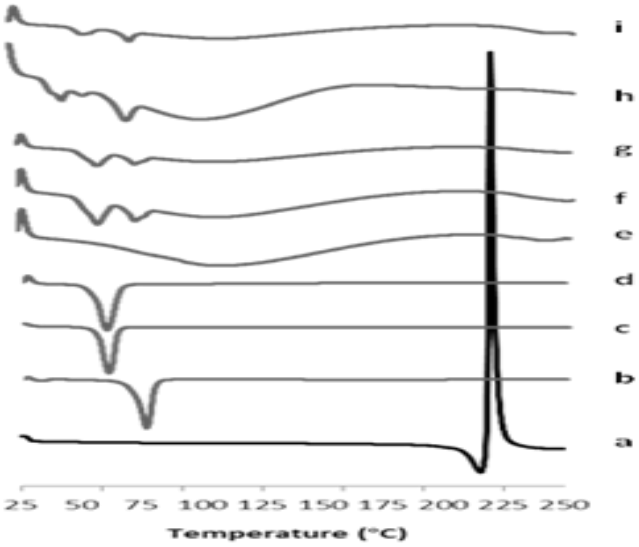

Figure 3: DSC characterization by heating (5ºC/min) of a. BM, b. tristearin, c. trimyristin, d. Pluronic F127, e. maltodextrin, f. physical mixture of a-e, g. cBMSLN powder, h. physical mixture of a-e with castor oil and i. cBMNLC powder.

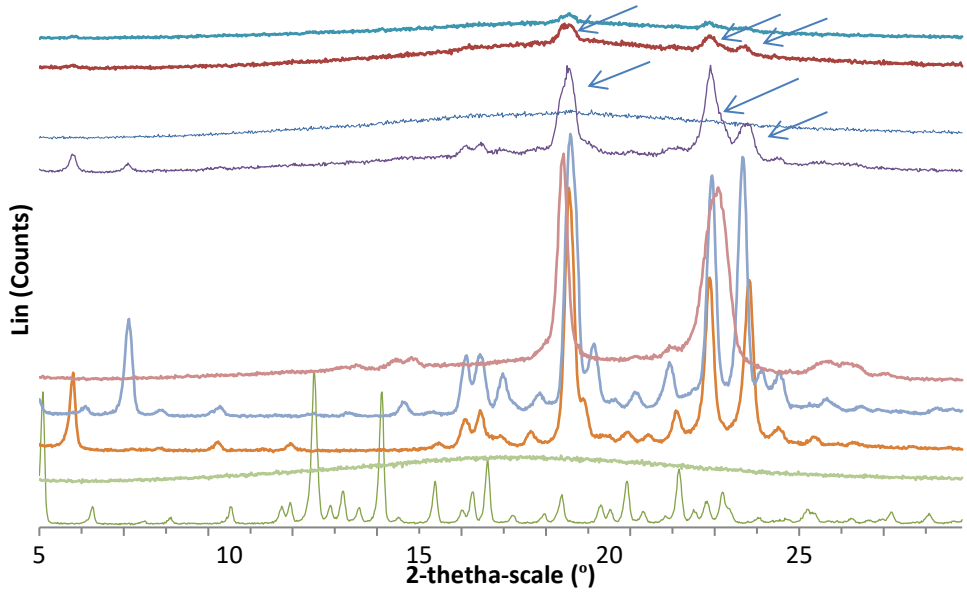

Figure 4: WXRD characterization a) BM, b) maltodextrin, c) tristearin, d) trimyristin, e) Pluronic f127, f) physical mixture of ingredients a-e, g. cBMSLN powder, h) physical mixture of ingredients a-e with castor oil and i) cBMNLC powder.

cBMNLC powder were mostly disappeared (Figures 4g and 4i) indicating that most components were in molecularly dispersion. Although melting at spray drying temperature, long chain triglycerides could overcome solidification problems[40]. However, rapid cooling to powder would inhibit recrystallization[41]. These amorphous powders could lead to better dispersion in GI tract.

Morphology and physical properties

Spray dried powders

The log-normal size distribution by volume plots and SEM photomicrographs of the spray dried powders from optimum conditions are shown in Figures 5a-5b, respectively, while Table 4 shows their physical characterization. Upon spray drying, all systems of BMSLN, cBMSLN, BMNLC and cBMNLC underwent spherical aggregation to micron size, *d*(4,3)=4-5 µm (Table 4), which was caused by high inlet temperature to melt and fuse the nanolipidic systems of tristearin (melting points of α, β*, β at 54.5, 64.3, 73.1 °C,) and trimyristin (melting points of α*, β*, β at 32.0, 44.0, 55.5 °C)[42] and formed nanoaggregates. Moreover, the properties of surfactant layer might change and reduce its repulsion and stabilization effects[43, 44].

The liquid lipid could round up during NLC powder formation resulting in smoother surface when compared to SLN systems. Adding chitosan resulted in rough, less porous and larger powder likely due to the increasing viscosity of dispersion systems[45].

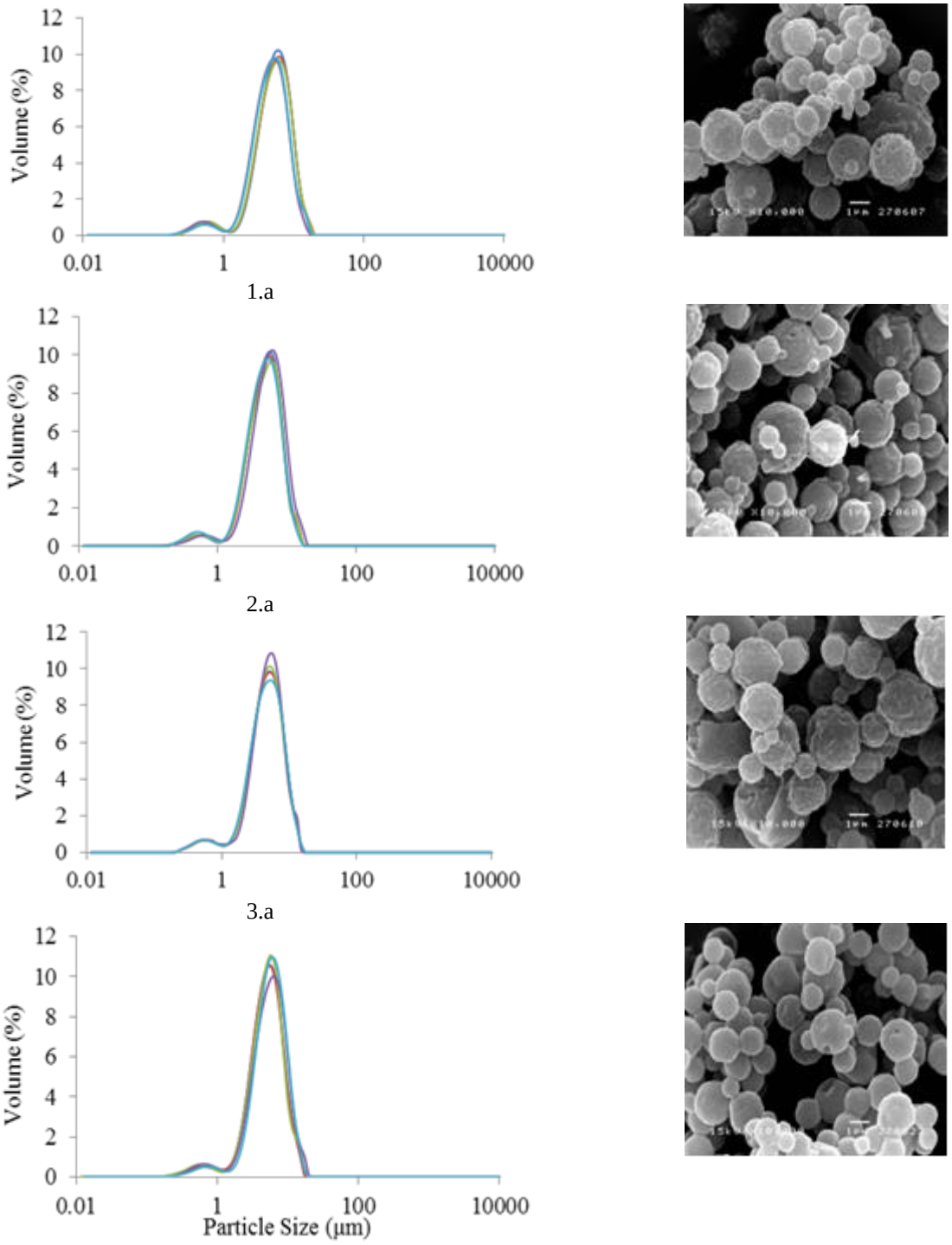

1.a

2.a

3.a

4.a

Figure 5: Log-normal size distribution by volume plots (a) and SEM characterization (b) of spray dried nanosystems of: 1) BMSLN, 2) cBMSLN, 3) BMNLC, 4) cBMNLC.

All powders had quite narrow bimodal volume size distribution according to the spraying droplets (Figure 5.1a-4a). Slight narrower volume size distributions of NLC powders indicated more uniformity. The span value indicating of homogeneity was the lowest in cBMNLC powder (Table 4).

Table 4 Powder yield, moisture content, mean volume size distribution, span and Carr's compressibility index (CI) of all obtained spray dried powders (mean ±SD, n=5)

The % powder yield was quite high of 65%-70%. Spray drying process on SLN systems was more effective than that on NLC systems. Incorporating chitosan rendered less powder yield with a slight increase in mean size due to adhesion property of the polymer and coating onto the particle surface, respectively. This adhesive effect also led to slightly poorer powder flowability observed from their higher CI values (Table 4). No significant difference was

Table 4: Powder yield, moisture content, mean volume size distribution, span and Carr's compressibility index (CI) of all obtained spray dried powders (mean ±SD, n=5).

Formulation	Yield (%)	Moisture Content %)	d(4,3) (µm)	span	CI
BMSLN	70.61±0.56	5.04±0.20	4.74±0.09	1.43±0.02	23.33±3.81
cBMSLN	68.21±0.78	5.40±0.27	4.99±0.24	1.44±0.05	26.67±3.81
BMNLC	68.45±2.26	5.17±0.82	4.77±0.07	1.44±0.06	25.00±2.50
cBMNLC	65.30±1.01	5.21±0.41	5.09±0.12	1.38±0.04	28.75±3.31

Table 5: Comparison of size, zeta potential (ZP), polydispersity index (PI), drug entrapment efficiency (DEE) and drug retention (DR) of SLN and NLC systems and their powder redispersions (mean (n=5) ±SD).

Formulation	Prepared solid lipid nanosystem				Powder redispersion			
	Size (nm)	ZP (mV)	PI	DEE (%)	Size (nm)	ZP (mV)	PI	DR (%)
BMSLN	112.70 ±3.56	-0.89 ±0.32	0.44 ±0.03	86.33 ±0.07	569.10 ±19.50	-7.37 ±0.31	0.37 ±0.07	22.87 ±0.61
cBMSLN	164.5 ±2.23	20.0 ±1.69	0.49 ±0.02	63.87 ±0.59	662.71 ±94.79	19.37 ±3.80	0.41 ±0.09	47.44 ±0.55
BMNLC	101.62 ±5.26	5.37 ±0.82	0.53 ±0.09	90.09 ±4.96	468.70 ±21.13	-9.41 ±1.57	0.41 ±0.11	46.12 ±1.38
cBMNLC	158.7 ±3.89	18.4 ±1.23	0.55 ±0.10	64.80 ±0.38	594.96 ±63.83	14.84 ±1.23	0.46 ±0.16	62.44 ±0.76

observed on their moisture content which was around 5% ($p<0.05$).

Size of redispersed nanoaggregates

The size distribution and TEM photomicrographs of both SLN and NLC systems including their redispersions, with and without chitosan are illustrated in Figure 6.1-6.2, respectively and their characterization are listed in Table 5. BMSLN and BMNLC possessed spherical with some oblong shape and nanometer size range (Figures 6.1a and 6.2a). After chitosan coating, the surface became smoother and more spherical (Figures 6.1b and 6.2b) with about 50 nm increment in particle size (Table 5). Their zeta potential was altered from almost neutral to positive values. Chitosan having positive charge would adhere to polysorbate 80 and neutral lipid by hydrogen bonding and hydrophobic interaction[46].

Spherical nanoaggregates were clearly seen after redispersion of the spray dried powders. Their smoothness and roundness were ranked: cBMSLN > BMSLN > cBMNLC > BMNLC (Fig 6.1d, 6.1c, 6.2d, 6.2c), respectively. Denser nanoaggregates were noticed in both SLN systems than in NLC systems indicating possibly less physical stability of latter systems. Larger size of nanoaggregates and slightly smaller PI of SLN systems than those of NLC systems were related to their original sizes and PI values (Table 5). In addition, slight decrease in zeta potential was noticed when compared to their original nanosystems.

Log-normal volume size distribution in Figure 6 reveals that all 4 redispersions had markedly larger size than their corresponding original nanosystems. The majority of both BMSLN and cBMSLN redispersions formed nanoaggregates with peak sizes at 412 and 477 nm, respectively, while those of NLC redispersions were at 265 and 412 nm, respectively. Smaller nanosize peak closed to their original size could also be noticed. The % volume distribution at these two peaks of both BMSLN and cBMSLN redispersions were 1.3%, 19.5% and 0.7%, 19.2%, respectively, while 5.8%, 18.6% and 3.7%, 17.8% were from BMNLC and cBMNLC redispersions, respectively.

Drug entrapment efficiency (DEE) and Drug retention (DR)

DEE in BMSLN and BMNLC were 86.33% and 90.09%, respectively (Table 5), indicating that the drug was well-entrapped into the lipid nanoparticles. Higher DEE value in BMNLC was due to castor oil in the formulation to increase drug loading and avoid drug expulsion during processing. Adding chitosan decreased DEE. The partition coefficient of BM was reported to be less at low pH than at high pH[47]. Chitosan in 1% of acetic acid expressed lower pH environment suggesting more drug leaking from lipid nanoparticles.

The DR of BMSLN and cBMSLN powders were 22.87% and 47.44%, respectively, while those from BMNLC and cBMNLC powders were 46.12%, and 62.44%, respectively (Table 5). BM is extremely unstable in association with light and heat[48], thus un-entrapped BM and the expulsed drug from lipid droplet would undergo rapid degradation after exposure to high inlet temperature. Although drug entrapment was lower in chitosan coated nanosystems, their drug retention was higher than uncoated systems. Gel property of chitosan obviously formed skin around the droplets which could absorb most of the heat, thus prevented drug degradation, avoided particle deformation, and retarded drug release or drug expulsion[37]. In addition, the hydrogen bond between hydroxyl group of chitosan and surfactant on these lipid particles might form a mechanical interlocking of long polymer chains that played role on impairing drug leaking[49].

Table 5 Comparison of size, zeta potential (ZP), polydispersity index (PI), drug entrapment efficiency (DEE) and drug retention (DR) of SLN and NLC systems and their powder redispersions (mean (n=5) ±SD)

Stability studies

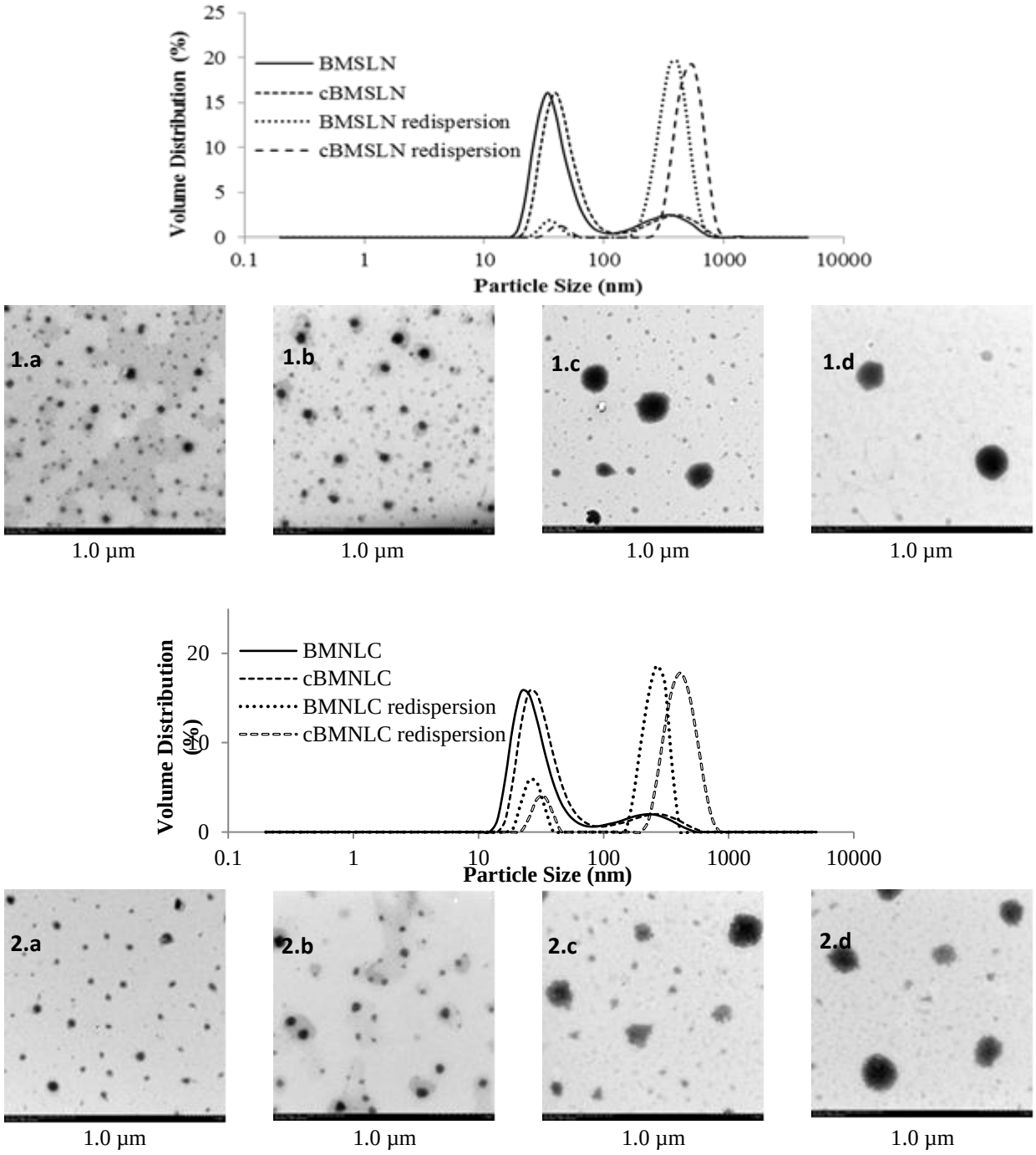

Figure 6: Log-normal size distribution by volume plots of BMSLN systems and their TEM characterization (1) and BMNLC systems and their TEM characterization (2): 1.a BMSLN, 1.b cBMSLN 1.c BMSLN redispersion, 1.d cBMSLN redispersion, 2.a BMNLC, 2.b cBMNLC, 2.c BMNLC redispersion, 2.d cBMNLC redispersion. Scale bars equal to 1.0 µm.

The drug content in chitosan coated lipid-based nanosystems and in capsules containing corresponding spray dried powders consequently and markedly decreased after 3 months at 25°C and was ranked: cBMSLN < cBMNLC < cBMSLN powder < cBMNLC powder (34.73%, 36.02%, 44.74% and 53.29%, respectively, (Figure 7). BM as salt (pKa = 4.96) is easily ionized and degraded when exposed to water[47]. Removing water from nanoparticles environment significantly reduced the deteriorative change in addition to impair drug leakage. However, unsatisfactory low drug stability in capsules was possibly due to some moisture content in spray dried powders (Table 4) that facilitated drug degradation. Better drug stability from NLC systems than SLN systems was also observed due to higher drug solubility in liquid lipid and less drug expulsion[50].

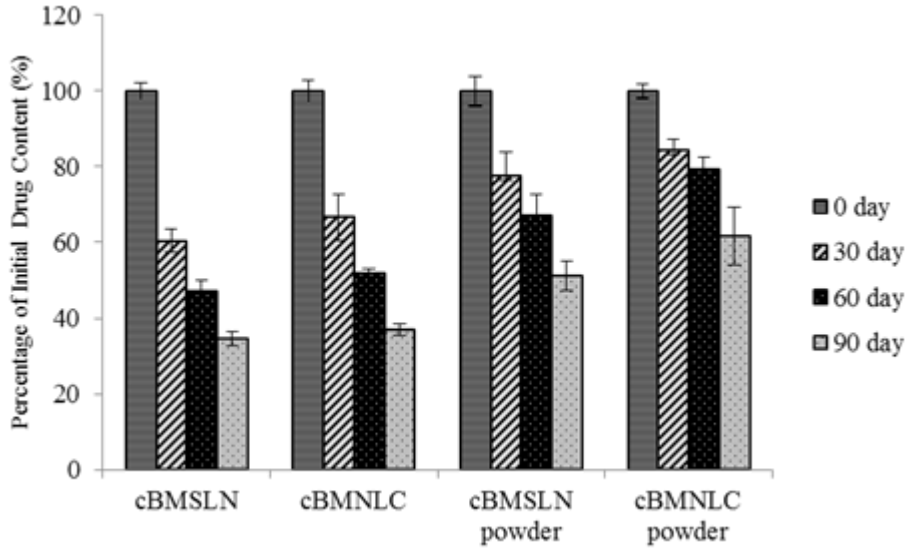

Figure 7: Drug content in various chitosan coated lipid-based nanosystems of bromocriptine mesylate after storage at 25±2°C upto 3 months. Error bars represent standard deviations of the mean based on three replicates (Powders were filled into capsules and packed in aluminum strips).\

CONCLUSIONS

Redispersible powder of cBMSLN could be successfully prepared by optimizing the spray drying parameters using response surface methodology and central composite rotatable design. The optimized spray drying conditions could further be employed to prepare powders of cBMNLC and nanosystems without chitosan. Amorphous characteristics were observed in all spray dried powders**.** The obtained micron-size powders rendered nanoaggregates upon redispersion in water by mild agitation with bimodal volume size distribution; small portion of similarly original nanosize and main portion of larger size. Chitosan obviously impaired drug degradation during spray drying. In addition, as dry powder, drug stability markedly improved. NLC systems were better lipid-based nanosystems than SLN systems in terms of producing smaller size of redispersed nanoaggregates, higher drug retention and better drug stability.

ACKNOWLEDGEMENT

This work has been supported by the National Research University Project of CHE and the Ratchadaphiseksomphot Endowment Fund (Project code HR1166I) and the Center of Innovative Nanotechnology, Chulalongkorn University.

REFERENCES

1. Kesisoglou F, Panmai S, Wu Y. Nanosizing — Oral formulation development and biopharmaceutical evaluation. Advanced Drug Delivery Reviews. 2007;59(7):631-44.
2. Hoffmeister CR, Durli TL, Schaffazick SR, Raffin RP, Bender EA, Beck RC, et al. Hydrogels containing redispersible spray-dried melatonin-loaded nanocapsules: a formulation for transdermal-controlled delivery. Nanoscale research letters. 2012;7(1):1-13.
3. Freitas C, Müller RH. Effect of light and temperature on zeta potential and physical stability in solid lipid nanoparticle (SLN™) dispersions. International journal of pharmaceutics. 1998;168(2):221-9.
4. Chaubal MV, Popescu C. Conversion of nanosuspensions into dry powders by spray drying: a case study. Pharmaceutical research. 2008;25(10):2302-8.
5. Thongrangsalit S, Phaechamud T, Lipipun V, Ritthidej GC. Bromocriptine tablet of self-microemulsifying system adsorbed onto porous carrier to stimulate lipoproteins secretion for brain cellular uptake. Colloids and Surfaces B: Biointerfaces. 2015;131:162-9.
6. Ribeiro RF, Motta MH, Härter APG, Flores FC, Beck RCR, Schaffazick SR, et al. Spray-dried powders improve the controlled release of antifungal tioconazole-loaded polymeric nanocapsules compared to with lyophilized products. Materials Science and Engineering: C. 2016;59:875-84.
7. Mu L, Feng S. Fabrication, characterization and in vitro release of paclitaxel (Taxol®) loaded poly (lactic-co-glycolic acid) microspheres prepared by spray drying technique with lipid/cholesterol emulsifiers. Journal of Controlled Release. 2001;76(3):239-54.
8. Saklatvala R, Royall PG, Craig DQ. The detection of amorphous material in a nominally crystalline drug using modulated temperature DSC—A case study. International journal of pharmaceutics. 1999;192(1):55-62.
9. Kakkar V, Singh S, Singla D, Kaur IP. Exploring solid lipid nanoparticles to enhance the oral bioavailability of curcumin. Molecular nutrition & food research. 2011;55(3):495-503.
10. Minagawa T, Sakanaka K, Inaba SI, Sai Y, Tamai I, Suwa T, et al. Blood-brain-barrier Transport of Lipid Microspheres Containing Clinprost, a Prostaglandin I2

Analogue. Journal of pharmacy and pharmacology. 1996;48(10):1016-22.
11. Blasi P, Giovagnoli S, Schoubben A, Ricci M, Rossi C. Solid lipid nanoparticles for targeted brain drug delivery. Advanced drug delivery reviews. 2007;59(6):454-77.
12. Müller R, Petersen R, Hommoss A, Pardeike J. Nanostructured lipid carriers (NLC) in cosmetic dermal products. Advanced drug delivery reviews. 2007;59(6):522-30.
13. Juliano RL. Factors affecting the clearance kinetics and tissue distribution of liposomes, microspheres and emulsions. Advanced Drug Delivery Reviews. 1988;2(1):31-54.
14. Wang J-X, Sun X, Zhang Z-R. Enhanced brain targeting by synthesis of 3′, 5′-dioctanoyl-5-fluoro-2′-deoxyuridine and incorporation into solid lipid nanoparticles. European Journal of Pharmaceutics and Biopharmaceutics. 2002;54(3):285-90.
15. Huang C, Zhang R, Chen Z, Jiang Y, Shang Z, Sun P, et al. Predict potential drug targets from the ion channel proteins based on SVM. Journal of theoretical biology. 2010;262(4):750-6.
16. Owens Iii DE, Peppas NA. Opsonization, biodistribution, and pharmacokinetics of polymeric nanoparticles. International Journal of Pharmaceutics. 2006;307(1):93-102.
17. Gelperina S, Maksimenko O, Khalansky A, Vanchugova L, Shipulo E, Abbasova K, et al. Drug delivery to the brain using surfactant-coated poly (lactide-co-glycolide) nanoparticles: influence of the formulation parameters. European Journal of Pharmaceutics and Biopharmaceutics. 2010;74(2):157-63.
18. Sarmento B, Mazzaglia D, Bonferoni MC, Neto AP, do Céu Monteiro M, Seabra V. Effect of chitosan coating in overcoming the phagocytosis of insulin loaded solid lipid nanoparticles by mononuclear phagocyte system. Carbohydrate polymers. 2011;84(3):919-25.
19. Kean T, Thanou M. Biodegradation, biodistribution and toxicity of chitosan. Advanced drug delivery reviews. 2010;62(1):3-11.
20. Tosi G, Costantino L, Ruozi B, Forni F, Vandelli MA. Polymeric nanoparticles for the drug delivery to the central nervous system. Expert opinion on drug delivery. 2008;5(2):155-74.
21. Luo Y, Teng Z, Li Y, Wang Q. Solid lipid nanoparticles for oral drug delivery: Chitosan coating improves stability, controlled delivery, mucoadhesion and cellular uptake. Carbohydrate Polymers. 2015;122:221-9.
22. Montgomery DC. Design and analysis of experiments: John Wiley & Sons; 2008.
23. Box GE, Hunter WG, Hunter JS. Statistics for experimenters. 1978.
24. Castelli F, Puglia C, Sarpietro MG, Rizza L, Bonina F. Characterization of indomethacin-loaded lipid nanoparticles by differential scanning calorimetry. International journal of pharmaceutics. 2005;304(1):231-8.
25. Suresh G, Manjunath K, Venkateswarlu V, Satyanarayana V. Preparation, characterization, and in vitro and in vivo evaluation of lovastatin solid lipid nanoparticles. AAPS PharmSciTech. 2007;8(1):E162-E70.
26. Chen J-P, Yang P-C, Ma Y-H, Wu T. Characterization of chitosan magnetic nanoparticles for in situ delivery of tissue plasminogen activator. Carbohydrate Polymers. 2011;84(1):364-72.
27. Podczeck F. Particle-particle adhesion in pharmaceutical powder handling: World Scientific; 1998.
28. Esposito E, Fantin M, Marti M, Drechsler M, Paccamiccio L, Mariani P, et al. Solid lipid nanoparticles as delivery systems for bromocriptine. Pharmaceutical research. 2008;25(7):1521-30.
29. Zhuang C-Y, Li N, Wang M, Zhang X-N, Pan W-S, Peng J-J, et al. Preparation and characterization of vinpocetine loaded nanostructured lipid carriers (NLC) for improved oral bioavailability. International journal of pharmaceutics. 2010;394(1):179-85.
30. Borhade V, Nair H, Hegde D. Design and evaluation of self-microemulsifying drug delivery system (SMEDDS) of tacrolimus. Aaps Pharmscitech. 2008;9(1):13-21.
31. Asasutjarit R, Lorenzen S-I, Sirivichayakul S, Ruxrungtham K, Ruktanonchai U, Ritthidej GC. Effect of solid lipid nanoparticles formulation compositions on their size, zeta potential and potential for in vitro pHIS-HIV-hugag transfection. Pharmaceutical research. 2007;24(6):1098-107.
32. Chen XD. Heat-mass transfer and structure formation during drying of single food droplets. Drying technology. 2004;22(1-2):179-90.
33. Goula AM, Adamopoulos KG. Spray drying performance of a laboratory spray dryer for tomato powder preparation. Drying Technology. 2003;21(7):1273-89.
34. Gallo L, Llabot JM, Allemandi D, Bucalá V, Piña J. Influence of spray-drying operating conditions on Rhamnus purshiana (Cáscara sagrada) extract powder physical properties. Powder Technology. 2011;208(1):205-14.
35. Cai Y, Corke H. Production and Properties of Spray-dried Amaranthus Betacyanin Pigments. Journal of food science. 2000;65(7):1248-52.
36. Hong JH, Choi YH. Physico-chemical properties of protein-bound polysaccharide from Agaricus blazei Murill prepared by ultrafiltration and spray drying process. International journal of food science & technology. 2007;42(1):1-8.
37. Mosén K, Bäckström K, Thalberg K, Schaefer T, Kristensen HG, Axelsson A. Particle formation and capture during spray drying of inhalable particles. Pharmaceutical development and technology. 2005;9(4):409-17.
38. Westesen K, Bunjes H. Do nanoparticles prepared from lipids solid at room temperature always possess a solid lipid matrix? International journal of pharmaceutics. 1995;115(1):129-31.

39. Wasutrasawat P, Al-Obaidi H, Gaisford S, Lawrence MJ, Warisnoicharoen W. Drug solubilisation in lipid nanoparticles containing high melting point triglycerides. European Journal of Pharmaceutics and Biopharmaceutics. 2013;85(3):365-71.
40. Bunjes H, Westesen K, Koch MH. Crystallization tendency and polymorphic transitions in triglyceride nanoparticles. International journal of pharmaceutics. 1996;129(1):159-73.
41. Zhang L, Liu L, Qian Y, Chen Y. The effects of cryoprotectants on the freeze-drying of ibuprofen-loaded solid lipid microparticles (SLM). European journal of pharmaceutics and biopharmaceutics. 2008;69(2):750-9.
42. Lutton E. The polymorphism of tristearin and some of its homologs. Journal of the American Chemical Society. 1945;67(4):524-7.
43. Lee K, Cho S, Lee H, Jeong S, Yuk S. Microencapsulation of lipid nanoparticles containing lipophilic drug. Journal of microencapsulation. 2003;20(4):489-96.
44. Tewa-Tagne P, Briançon S, Fessi H. Preparation of redispersible dry nanocapsules by means of spray-drying: development and characterisation. European Journal of Pharmaceutical Sciences. 2007;30(2):124-35.
45. Mi FL, Wong TB, Shyu SS, Chang SF. Chitosan microspheres: modification of polymeric chem-physical properties of spray-dried microspheres to control the release of antibiotic drug. Journal of Applied Polymer Science. 1999;71(5):747-59.
46. Luo Q, Zhao J, Zhang X, Pan W. Nanostructured lipid carrier (NLC) coated with Chitosan Oligosaccharides and its potential use in ocular drug delivery system. International journal of pharmaceutics. 2011;403(1):185-91.
47. Giron-Forest D, Schanleber W. Analytical Profiles of Drug Substances. Academic Press, New York; 1992.
48. Florey K. Profiles of drug substances, excipients and related methodology: Academic press; 1983.
49. Learoyd TP, Burrows JL, French E, Seville PC. Chitosan-based spray-dried respirable powders for sustained delivery of terbutaline sulfate. European journal of pharmaceutics and biopharmaceutics. 2008;68(2):224-34.
50. Wissing S, Kayser O, Müller R. Solid lipid nanoparticles for parenteral drug delivery. Advanced drug delivery reviews. 2004;56(9):1257-72.